



Horizon 2020 Societal challenge 5:
Climate action, environment, resource
efficiency and raw materials

VERIFY

Observation-based system for monitoring and verification of greenhouse gases

GA number 776810, RIA

Deliverable number (relative in WP)	D3.12
Deliverable name:	Second Complete NEE inversions
WP / WP number:	WP3
Delivery due date:	Month 30 (31/07/2020)
Actual date of submission:	Month 33 (23/10/2020)
Dissemination level:	Public
Lead beneficiary:	MPG
Responsible	Christoph Gerbig
Contributor(s):	Saqr Munassar
Internal reviewer:	Matthew McGrath

Changes with respect to the DoA
None.
Dissemination and uptake (Who will/could use this deliverable, within the project or outside the project?)
The inversion results are freely available from the VERIFY database (with password protection, available from the PI or the VERIFY coordination team). The results include a priori fluxes (used as initial guess) and posterior fluxes (optimized using atmospheric observations) to be used in the synthesis product in WP5. The web-page for data download is listed in section 3.
Short Summary of results (<250 words)
<p>Biosphere-atmosphere exchange of CO₂ and its interaction with climate drivers is an important player in the carbon cycle. To estimate net ecosystem exchange (NEE) fluxes, VERIFY includes both biospheric models for bottom-up estimation of fluxes and a regional inversion for a top-down estimation.</p> <p>The Jena CarboScope-Regional (CSR) inversion system has been deployed for the 2006-2019 period to estimate biosphere-atmosphere exchange fluxes from the top-down perspective, using recent atmospheric observations up to 2019. This deliverable provides details about the inversion. The results include a priori fluxes (used as initial guess) from the diagnostic light use efficiency model VPRM and FLUXCOM model, and posterior fluxes from the CSR inversion. <i>A priori fluxes from the ORCHIDEE model will be used upon their reception from LSCE (before the end of 2020).</i></p>
Evidence of accomplishment (report, manuscript, web-link, other)
All the simulation results are accessible through the dedicated data THREDDS server: https://verifydb.lsce.ipsl.fr/thredds/catalog/verify/WP3/catalog.html

Version	Date	Description	Author (Organisation)
V0	1/07/2020	Creation/Writing	Christoph Gerbig (MPI-BGC)
V0.1	15/07/2020	Writing/Formatting/Delivery	Christoph Gerbig (MPI-BGC) Philippe Peylin (CEA)
V1	23/10/2020	Formatting/Delivery on the Participant Portal	Matthew McGrath, Aur�lie Paquirissamy (CEA)

1. Glossary	5
2. Introduction	6
3. Setup	7
3.1. Regional transport model	7
3.2. Spatial domain and state space	7
3.3. A priori fluxes	7
3.3.1. Biosphere-atmosphere exchange	7
3.3.2. Fossil fuel emissions	8
3.3.3. Ocean fluxes.....	8
3.4. Atmospheric observations.....	8
3.5. Lateral boundary condition	9
4. Results	10
4.1. NEE for 2019 in context of the 2006-2018 period.....	10
4.2. Sensitivity runs.....	13
4.2.1. IAV test.....	13
5. Conclusions	14
6. References	15

1.Glossary

Abbreviation / Acronym	Description/meaning
CSR	Jena CarboScope-Regional inversion system
ECMWF	European Centre for Medium-Range Weather Forecasts
IAV	interannual variations
LBC	lateral boundary conditions
NEE	net ecosystem exchange
STILT	Stochastic Time Inverted Lagrangian Transport
TNO	Netherlands Organisation for Applied Scientific Research
VPRM	Vegetation Photosynthesis and Respiration Model

2.Introduction

This report describes the NEE inversions for the year 2019 using the Jena CarboScope-Regional (CSR) inversion system. The CSR system uses the combination of the regional transport model STILT (Stochastic Time Inverted Lagrangian Transport) and the global TM3 model. Surface-atmosphere fluxes are estimated from atmospheric observations of CO₂ mole fractions using the two-step scheme (Rödenbeck et al., 2009), consisting of a global inversion to provide lateral tracer transport to the regional domain, followed by a regional inversion.

Given that this is the first time that top-down constrained biosphere-atmosphere fluxes have been produced that cover such a recent period (up to the end of last year), many things had to be optimized such that the results can be obtained as soon as the observations become available. This made it impossible to implement at the same time some other features, such as the use of a priori biosphere-atmosphere exchange fluxes from the various bottom-up estimates produced within WP3 (which just became available), or the use of anthropogenic emission data from WP2. A couple of inversion runs using different a-priori flux models have been implemented within 3 biosphere models and 2 ocean flux models. In addition, 3 subsets of stations using total, core, and full-coverage sites were used in a different sensitivity test.

Results suggest that NEE estimates show a lesser uptake in 2019 over the European domain in the context of the 2006-2018 period, in particular in comparison with 2018 NEE estimates. 2018 has been characterized with a distinct drought event as has been explained in (Rödenbeck et al. 2020; Thompson et al. 2020). This domain-integrated weaker uptake is robust against using different sets of stations, including e.g. a subset of only 16 stations with consistent coverage during 2015-2019. Contrastingly, a larger uptake in 2019 was found over certain regions in central and north Europe such as Finland, France, and Sweden, which were affected by the drought in 2018.

3.Setup

3.1. Regional transport model

The regional transport model STILT (Stochastic Time Inverted Lagrangian Transport) driven by ECMWF meteorological fields from short-term forecasts from the IFS at 3-hourly and $0.2^\circ \times 0.2^\circ$ spatial resolution was used to pre-compute footprints for every atmospheric observing site at hourly resolution. STILT includes turbulent transport as well as vertical transport through convective clouds. Backward transport was simulated for 10 days, giving ample time for the regional domain to be flushed by advection. The temporal resolution of each footprint was also one hour, sufficient to fully resolve the coupling between transport and fluxes. The spatial resolution of the footprints is $0.25^\circ \times 0.25^\circ$.

3.2. Spatial domain and state space

The CarboScope-Regional inversion system was set up for a European domain covering 33N - 73N in latitude and 15W – 35E in longitude. The full inversion period covers the years 2006 – 2019. The spatial resolution is $0.25^\circ \times 0.25^\circ$, and the temporal resolution is hourly for the coupling between fluxes and transport.

The state space (or control vector), i.e. the variables optimized within the inversion, are additive flux corrections to prior fluxes at a spatial resolution of $0.5^\circ \times 0.5^\circ$ and a temporal resolution of three hours. A prior error structure was chosen following Kountouris et al. (2018) using a prior uncertainty at annual and domain-wide scale of 0.44 GtC/yr. The prior uncertainty uses spatial correlations with a length-scale of 100 km in a hyperbolic decay and temporal correlations with a time scale of 1 month.

3.3. A priori fluxes

3.3.1. Biosphere-atmosphere exchange

CarboScope-Regional uses biogenic prior CO_2 fluxes derived from the Vegetation Photosynthesis and Respiration Model, VPRM (Mahadevan et al., 2008). This diagnostic model uses ECMWF (European Centre for Medium-Range Weather Forecasts) operational meteorological data for radiation (downward shortwave radiative flux) and temperature (T2m), the SYNMAP land cover classification (Jung et al., 2006), and EVI (enhanced vegetation index) and LSWI (land surface water index) derived from MODIS surface reflectance products. Model parameters were optimized for Europe using eddy covariance measurements made during 2007 from 47 sites (Kountouris et al., 2015). VPRM NEE fluxes have been produced at a 0.25° degree spatial and hourly temporal resolution.

FLUXCOM is also used as a prior fluxes model in the CSR system providing hourly fluxes at 0.50° degree of spatial resolution (Jung et al. 2019). The product is based on a machine learning mechanism that combine energy flux measurements from eddy covariance sites, remote sensing (MODIS) and meteorological data. .

3.3.2. Fossil fuel emissions

Anthropogenic emissions from fossil fuel combustion are not optimized in the inversion, but are prescribed in the inversion and treated as fixed boundary conditions. They are taken from EDGARv4.3 fuel type and category specific emissions provided by Greet Janssens-Maenhout (EU-JRC), combined with information on national totals from fuel consumption data in recent years as compiled in the BP statistics 2019 (BP 2019), following the COFFEE approach (Steinbach et al., 2011). In addition, the temporal variations (diurnal, i.e. hour to hour, and seasonal, i.e. month to month) for different categories from the MACC-TNO report (Denier van der Gon et al., 2011) were used. This way diurnal, day of week, and seasonal variations from TNO as well as interannual variations from BP are included, providing hourly fluxes at the 0.25-degree resolution. The gridded TNO emissions from WP2 are not yet being used, but plans are to do that soon.

3.3.3. Ocean fluxes

Ocean fluxes in CarboScope-Regional are taken from Mikaloff-Flechter et al. (2007). Since the spatial domain in this project does not contain large areas covered with ocean, ocean fluxes are not adjusted in the inversion but are instead prescribed. This is, apart from the larger domain, the only difference between the CSR setup in this project and that described in Kounouris et al. (2018). Ocean fluxes from pCO₂-based CarboScope ocean flux product are also used as an alternative product at 5 x 4 degree of spatial resolution with 6-hourly fluxes to investigate the impact of changing ocean fluxes on NEE estimates.

3.4. Atmospheric observations

Atmospheric observations for the 2017-2019 inversion were taken from the dataset collected through the ICOS site network and provided by the ATC (M. Ramonet) on July 2, 2020. This includes a pre-release of ICOS data, and data from 23 sites and 6 non-ICOS sites stations within the CSR domain were used for 2019 while data from 44 sites from the drought data set were combined for years before. Of these stations, 22 are tall towers, nine coastal stations, eight mountain sites, six short towers or near-surface continental sites, and one station is classified as an urban neighborhood. Four new sites are added in 2019 from Germany; three of them towers (Karlsruhe, Steinkimmen, and Torfhaus) and one mountain site (Ochsenkopf). For tall towers, near-surface or coastal stations, 11:00-16:00 UTC observations (referring to the beginning of the observational hour) were used, while for mountain stations the observations from 23:00-04:00 UTC were used.

A model-data mismatch was assumed to be 1.5 ppm for tall towers, coastal and mountain sites, 2.0 ppm for ground based continental sites, and 4.0 ppm for stations in an urban neighborhood. These refer to uncertainties for weekly averages; for hourly data an error inflation was applied, for example in the case of tall towers the 1.5 ppm mismatch was inflated by the square root of the number of observations per week (42), resulting in 9.7 ppm for hourly data.

3.5. Lateral boundary condition

Lateral Boundary Conditions (LBCs) have been updated to encompass 2019 using the global model TM3 in the Carboscope inversion system to provide far field contributions of CO₂ to the regional domain of Europe. This is performed using the two-step scheme inversion approach (Rödenbeck et al., 2009) which makes use of both gridded global model at coarse resolution of 5 x 4 degrees and the regional model STILT at fine spatial resolution of 0.25 x 0.25 degree.

4.Results

4.1. NEE for 2019 in context of the 2006-2018 period

Posterior NEE (Fig. 4.1.1) fluxes estimated using two biosphere models (VPRM and FLUXCOM) show a larger biospheric source for 2019 compared to the prior NEE of both models.

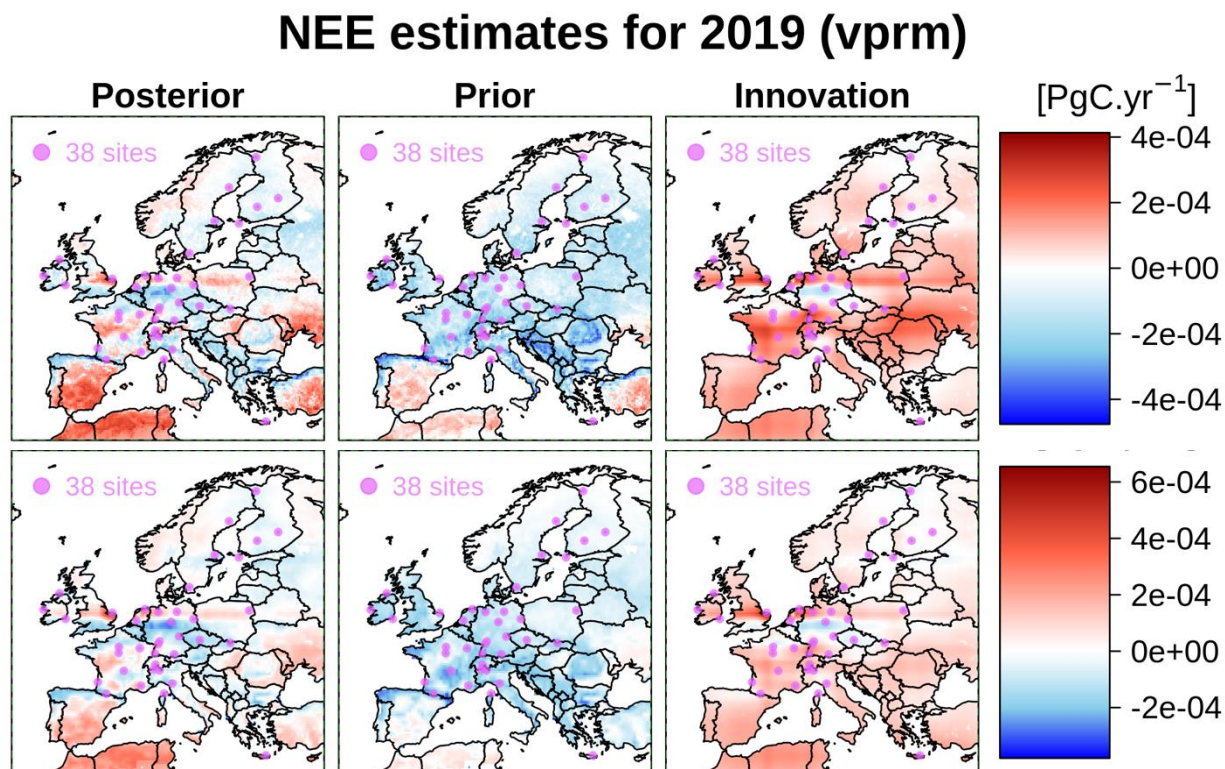


Figure 4.1.1: Annually integrated posterior NEE for 2019 from VPRM (top) and from FLUXCOM (bottom). Purple dots indicate the atmospheric observing stations used in the inversion.

NEE estimates for 2018 (vprm)

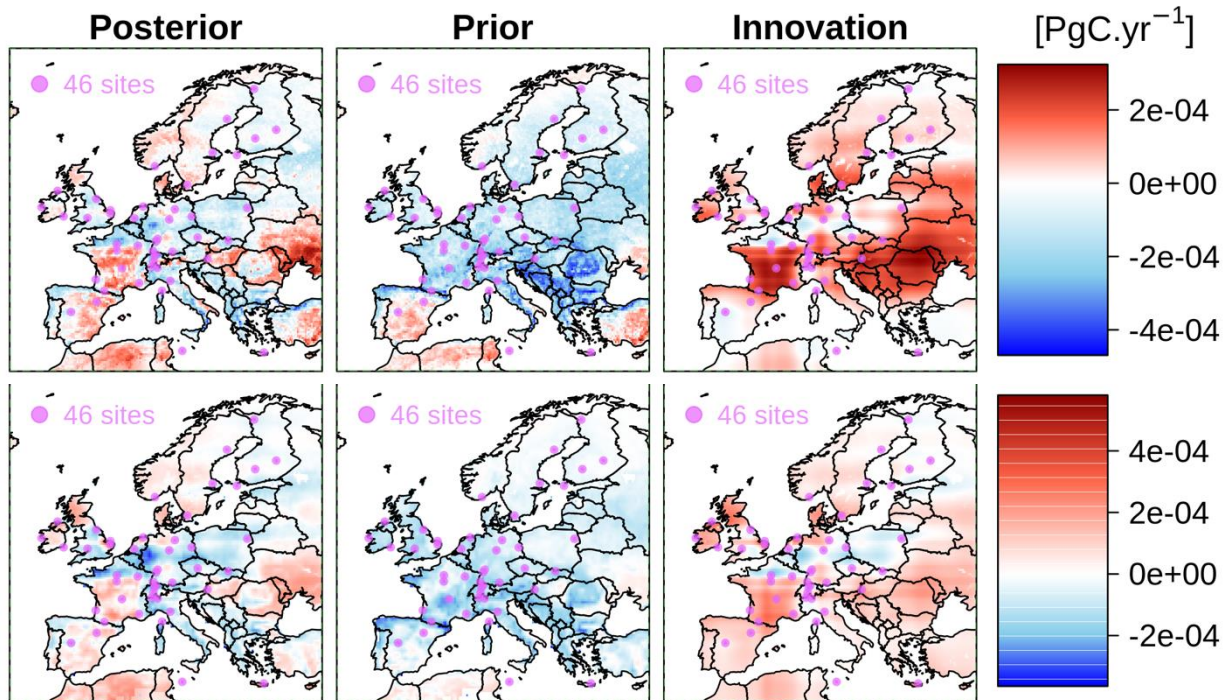


Figure 4.1.2: Same as Fig. 4.1.1 but for 2018 NEE

In order to put the year 2019 in context of a longer time period, results from the 2006-2018 CSR inversion using the two-step scheme are also shown.

NEE estimates for 2006-2019

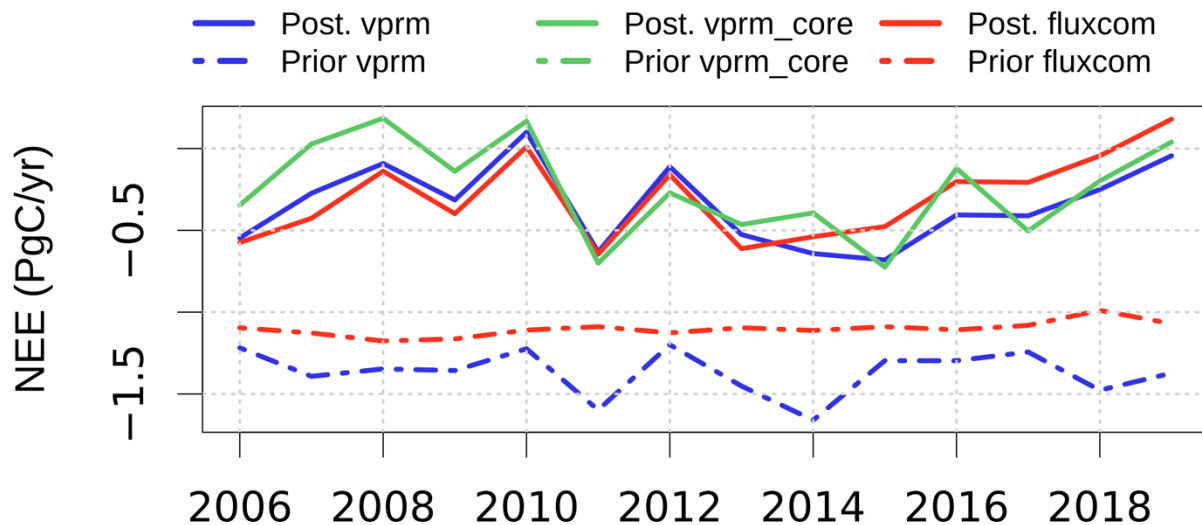


Figure 4.1.3. Annual domain-wide integrated NEE for the period 2006 – 2019. Priors are shown as dashed lines, posterior as solid lines. Different colors show results for different prior flux products used in the inversion.

Details for different regions as well as the corresponding prior and posterior uncertainties can be found in Fig. 4.1.4. NEE estimated using VPRM and FLUXCOM suggests good agreement, not only

over the full domain but also for subregions and countries. The posterior uncertainty range, indicated by the red shading, shows a notable reduction relative to prior uncertainty (in grey shading). The more the stations installed in a region the larger the uncertainty reduction is. For example, central Europe and France show quite a consistent a-posteriori variability and have very small uncertainty as a result of strong atmospheric signal and weak dependency on prior fluxes. In contrast, a weak atmospheric constraint leads to a large posterior variability as can be noticed over Turkey, where no atmospheric observations are available. The impact of datasets can also be observed from the decreasing posterior uncertainty in recent years at regions that have a growing number of stations, in particular in northern Europe and its underlying regions such as Finland, Sweden, and Norway.

It is obvious that the interannual variations seen in the posterior fluxes from the 2006-2019 inversions are largely data-driven regardless of which prior flux models used. An additional test on the impact of prior interannual variability on the posterior variations was done using climatological VPRM fluxes, presented in the next section.

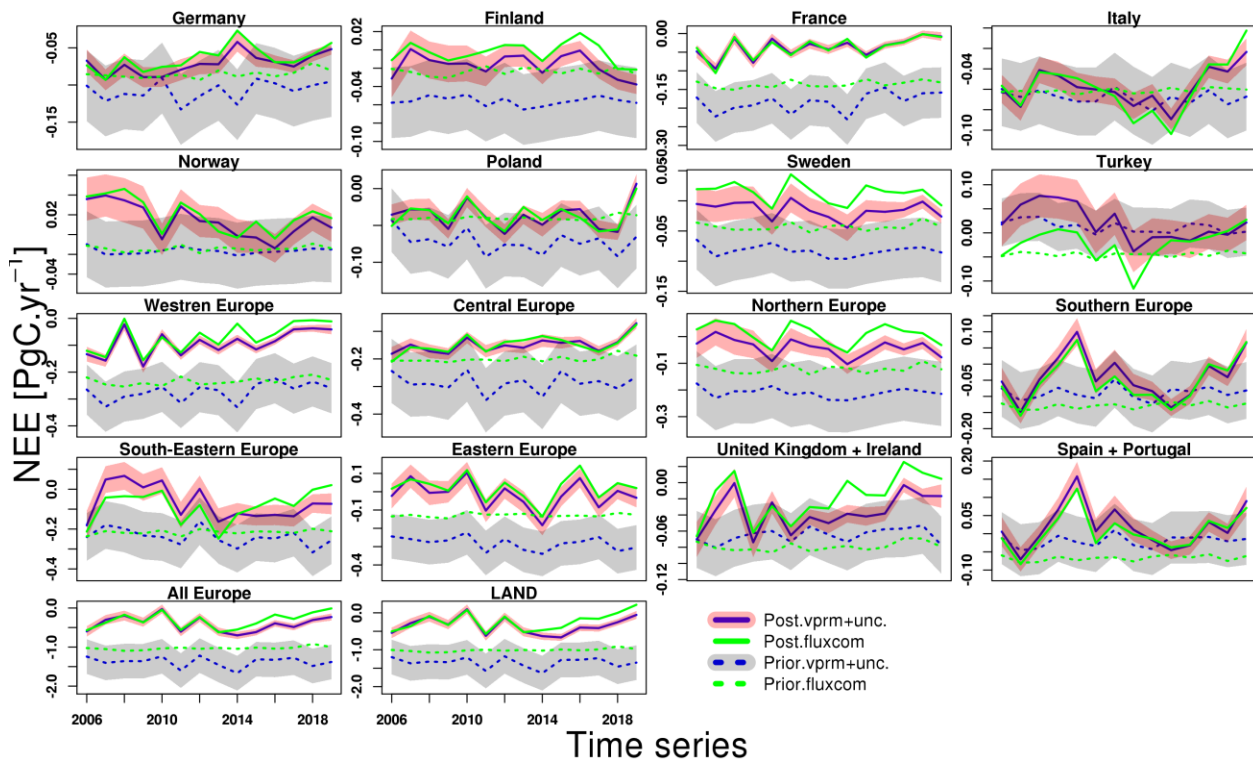


Figure 4.1.4. Annual NEE for the period 2006 – 2019 for different countries and partial domains using the EUROCOM region specifications. Prior fluxes from FLUXCOM are shown in dashed green and their corresponding posterior fluxes in solid green lines. Prior fluxes from VPRM are shown in dashed blue lines associated with uncertainties in grey shading, their posterior fluxes are in solid blue associated with uncertainties in red shading.

4.2. Sensitivity runs

4.2.1. IAV test

To assess whether interannual variations in posterior fluxes are dominated by interannual variations (IAV) in prior fluxes or rather by the atmospheric signal, an inversion was setup to use specifically filtered prior fluxes without IAV for the time period 2006 - 2018. Note that a different filter method was used than in the 2019 report D3.11: rather than using a Gaussian filter that removes IAV, we now used a filter that preserves exactly the hourly and day-to-day variations within each month, but monthly mean fluxes are forced to match the multi-year averaged monthly variations over the year. Results in Fig. 4.2.1 show that posterior fluxes exhibit IAV that show a similar behavior as those from the standard inversion using unfiltered VPRM fluxes. This confirms that the top-down constraint on interannual flux variations from the atmosphere is certainly dominant regardless of interannual variations in prior fluxes. This has also been emphasized in another test using de-seasonalized climatological fluxes. Of note that the interannual variability of VPRM (annually aggregated, left in Fig. 4.2.1) agrees quite well with the posterior variability from 2006 to 2015, albeit they disagree for individual months (e.g. much too small interannual variability in VPRM for January, middle in 4.2.1), and in total NEE with a substantial low bias in VPRM compared to the posterior estimates.

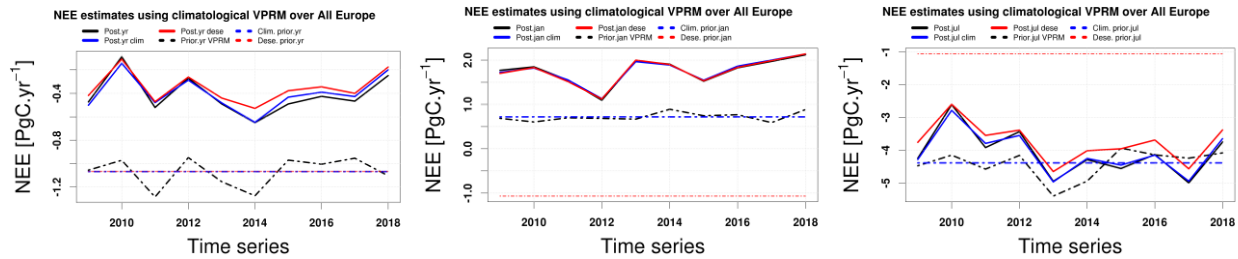


Figure 4.2.1: From left to right: annual, January, and July NEE estimates integrated domain-wide for 2009-2018 from a-priori VPRM (black dashed line), a-priori filtered to remove interannual variations (blue dashed line), and a-priori filtered to remove interannual and seasonal variations (red dashed line); their posterior fluxes are given by the same color but using solid lines.

5.Conclusions

Inversion results for 2019 NEE fluxes for the European domain have been obtained using the Jena CarboScope-Regional inversion framework, and put into the context of NEE in the 2006-2018 timeframe. The far field contribution to the regional domain of Europe is calculated through a global inversion run within the two-step scheme approach (Rödenbeck et al., 2009). In addition to drought data used in estimating 2018 NEE, a pre-release of observational data for 2019 provided by the ICOSATC was also included. So far, these datasets cover 29 sites, including 6 non-ICOS sites in 2019.

The NEE estimates of 2019 suggest a lower uptake of CO₂ over the full domain, leading to a slightly larger source than during the drought year 2018. However, the 2019-2018 difference in NEE estimates is also affected by the large difference in number of stations used in 2019 and 2018, 29 and 44 respectively. This leads to a weaker constraint in 2019 and in particular in regions with fewer observations. Meanwhile, NEE estimates over certain regions such as France, the UK, and North Europe show a larger uptake in 2019 compared to 2018. This finding is confirmed in an inversion run using a subset of stations having a consistent coverage over the years 2015-2019. The NEE estimates of 2019 are likely to be updated once observational data from other stations become available. In addition, we are planning on using a prior biogenic fluxes from the ORCHIDEE model run specifically for the VERIFY project at relatively high resolution (0.125 degrees) and ending in the year 2019 as soon as such results become available (before the end of 2020).

6. References

- BP, Statistical Review of World Energy, <https://www.bp.com/content/dam/bp/business-sites/en/global/corporate/xlsx/energy-economics/statistical-review/bp-stats-review-2019-all-data.xlsx>, 2019
- Denier van der Gon, H., Hendriks, C., Kuenen, J., Segers, A., Visschedijk, A.: TNO Report. Description of current temporal emission patterns and sensitivity of predicted AQ for temporal emission patterns EU FP7 MACC deliverable report D_D-EMIS_1.3,
- Kountouris, P., Gerbig, C., Rödenbeck, C., Karstens, U., Koch, T. F., and Heimann, M.: Atmospheric CO₂ inversions on the mesoscale using data-driven prior uncertainties: quantification of the European terrestrial CO₂ fluxes, *Atmos. Chem. Phys.*, 18, 3047–3064, <https://doi.org/10.5194/acp-18-3047-2018>, 2018.
- Kountouris, P., Gerbig, C., Totsche, K.-U., Dolman, A. J., Meesters, A. G. C. A., Broquet, G., Maignan, F., Gioli, B., Montagnani, L., and Helfter, C.: An objective prior error quantification for regional atmospheric inverse applications, *Biogeosciences*, 12, 7403–7421, <https://doi.org/10.5194/bg-12-7403-2015>, 2015.
- Mikaloff-Flechter, S. E., Gruber, N., Jacobson, A. R., Doney, S. C., Dutkiewicz, S., Gerber, M., Gloor, M., Follows, M., Joos, F., Lindsay, K., Menemenlis, D., Mouchet, A., Müller, S. A., and Sarmiento, J. L.: Inverse estimates of the oceanic sources and sinks of natural CO₂ and the implied oceanic transport, *Global Biogeochem. Cy.*, 21, GB1010, <https://doi.org/10.1029/2006GB002751>, 2007.
- Steinbach, J, C Gerbig, C Rödenbeck, U Karstens, C Minejima, and H Mukai: The CO₂ Release and Oxygen Uptake From Fossil Fuel Emission Estimate (COFFEE) Dataset: Effects From Varying Oxidative Ratios, *Atmospheric Chemistry and Physics* 11 (14): 6855–70. doi:10.5194/acp-11-6855-2011, 2011.
- Rödenbeck, C., Gerbig, C., Trusilova, K., and Heimann, M.: A two-step scheme for high-resolution regional atmospheric trace gas inversions based on independent models, *Atmos. Chem. Phys.*, 9, 5331–5342, <https://doi.org/10.5194/acp-9-5331-2009>, 2009.
- Jung, M., S. Koirala, U. Weber, K. Ichii, F. Gans, G. Camps-Valls, D. Papale, C. Schwalm, G. Tramontana, and M. Reichstein. 2019. 'The FLUXCOM ensemble of global land-atmosphere energy fluxes', *Sci Data*, 6: 74.
- Rodenbeck, C., S. Zaehle, R. Keeling, and M. Heimann. 2020. 'The European carbon cycle response to heat and drought as seen from atmospheric CO₂ data for 1999-2018', *Philos Trans R Soc Lond B Biol Sci*, 375: 20190506.
- Schaefer, Kevin, G. James Collatz, Pieter Tans, A. Scott Denning, Ian Baker, Joe Berry, Lara Prihodko, Neil Suits, and Andrew Philpott. 2008. 'Combined Simple Biosphere/Carnegie-



Ames-Stanford Approach terrestrial carbon cycle model', *Journal of Geophysical Research*, 113.

Thompson, R. L., G. Broquet, C. Gerbig, T. Koch, M. Lang, G. Monteil, S. Munassar, A. Nickless, M. Scholze, M. Ramonet, U. Karstens, E. van Schaik, Z. Wu, and C. Rodenbeck. 2020. 'Changes in net ecosystem exchange over Europe during the 2018 drought based on atmospheric observations', *Philos Trans R Soc Lond B Biol Sci*, 375: 20190512.